THE ARCHIVE OF MECHANICAL ENGINEERING

Vol. XLIX 2002 Number 2

Key words: *stabilising and tracking control system, tank gun stabiliser*

KRZYSZTOF M. PAPLIŃSKI[*)]

EXPERIMENTAL INVESTIGATIONS AND IDENTIFICATION OF A STABILISING AND TRACKING CONTROL SYSTEM

The subject of discussion is a tank gun horizontal stabiliser. In order to simplify identification, the system was divided into appropriate functional parts. Then, via laboratory tests, dynamic and static characteristics of those parts were obtained, and numerical values of coefficients of suitable mathematical model of the system were determined. The structural scheme of the overall system was derived on the basis of the obtained static characteristics and transfer functions of individual parts of the system, and based on the knowledge about the system feedbacks. For the investigation of the considered control system, one applied a method of computer simulations. The mathematical model and its numerical implementation was experimentally verified. To this aim:

- the results of model testing (for open-loop system) were compared with the existing results of experimental tests carried-out on a real tank;
- tests of the complete closed-loop system were carried -out and their results were compared with the results of numerical computations.

The results of experimental and model simulation investigations showed that the mathematical model and its numerical implementation was worked-out correctly.

1. Introduction

The considered military tank consists of three separate rigid bodies: the hull, the turret and the main gun (Fig. 1). The main gun must elevate relative to the turret, and the turret must rotate relative to the hull. The turret is rotated in yaw relative to the hull by the azimuth drive system. A d.c. motor, fixed to the turret, drives a gear box which contains an output pinion that drives a ring fixed in the hull. The gun is rotated in pitch relative to the turret by the elevation drive system. A hydraulic servo-motor, fixed to the gun and turret, drives the gun [1], [2].

Angular and axial displacements of the vehicle are the input signals acting on

[*)] *Military University of Technology, Institute of Motor Vehicles, 01-908, Warsaw, Kaliskiego 2, Poland; Phone: (0-22) 6839276, fax: (0-22) 6837370, E-mail: kpaplinski@wme.wat.waw.pl*

the turret and on the gun. The two-axial stabilisation system compensates the velocities of the vehicle. The stabilisation system automatically maintains a position of the gun at a fixed bearing in space. In spite of any motion of the vehicle in roll (γ), in pitch (ϕ) or in yaw (ψ), the tank gun stabiliser minimises the effects of vehicle motion on the main armament of the tank under typical conditions of tank operation over rough ground [3], [4].

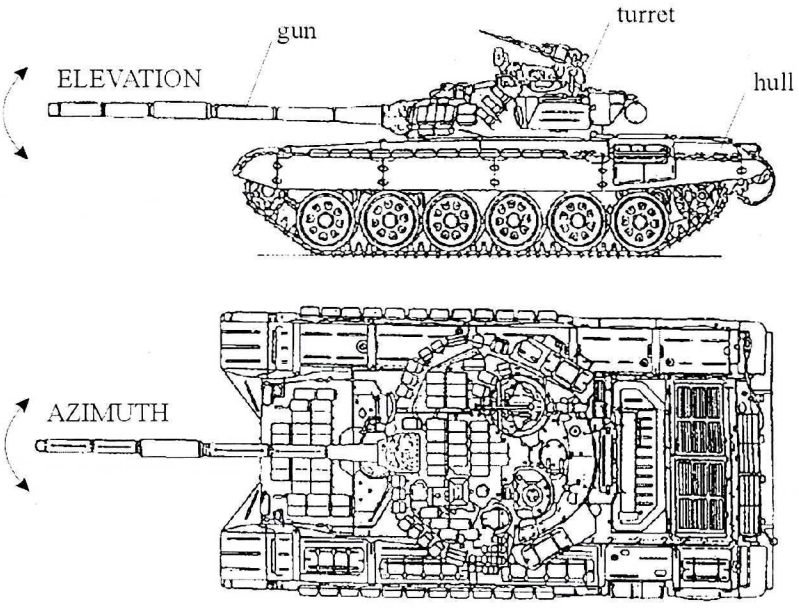

Fig. 1. Bodies of main battle tank

In the late forties, the British Army decided to introduce the first successfully stabilised gun control system on the newly developed then Centurion tanks. This system has now seen more than a quarter of a century of service in the Centurions and, what is more, has served as a model for the systems which later were produced in Britain, for the Chieftain and Vickers battle tanks, and in India for the Vijayanta battle tank. The systems developed for Centurions and for their successors have all been of the all-electric type and have provided stabilisation in both elevation and azimuth. In consequence, they incorporated two rate gyroscopes, mounted on the gun cradle.

A different line of development has been followed by the Soviet Army. It started in the early fifties with the T-54 tanks, whose guns were at first stabilised in elevation only. The more recent T-55 and T-62 tanks also had their turrets stabilised in azimuth, but they differ from all other tanks because of application of hybrid drive systems. These consist of an all-electric traverse (azimuth) drive for the turret and an electro-hydraulic elevation drive, which is

believed to have been developed later and to have been added to the earlier, electric traverse drive.

The stabilisation systems of T-55 and T-62 tanks are also different from that of other tanks. Thus, in each axis, they have a primary closed loop with a rate integrating gyro and a second, feed forward, open loop with a rate gyro (a block diagram of the turret drive is shown in Fig. 2). In principle, they are superior to the basic systems, but they are more expensive, not only because they incorporate four, instead of two gyros, but also because two of the gyros are of the rate integrating type and not of the more common rate type [1], [4], [5].

2. Functional scheme of elevation stabiliser

The T-55 battle tanks are equipped with STP-2 two-axis tank gun stabiliser [1], [3]. The subject of investigations is the tank gun stabiliser in horizontal plane (azimuth or traverse stabiliser). It is an electro-mechanical control system and it makes possible aiming at a target, tracking of a target and stabilising of a given gun angular position.

The tank gun drive in a main battle tank must be sufficient to enable the gunner to traverse the main armament quickly, track the target and undertake the fine lay onto the target. Traversing main armament normally requires the drive to work at a high speed, while tracking and final laying are operations requiring a lower, but steadier speed.

The power for the drive is taken from the onboard 24V supply system. The power is taken from the engine generator buffered over a set of batteries. It is fed to the electric motor (Fig. 2) [6]. This electric motor in turn drives an amplidyne (180V generator). The electric d.c. motor (turret drive) is fed by the amplidyne. An electronic control unit compares the actual speed of the drive with the speed specified by the gunner, and regulates the system setting accordingly to compensate for any discrepancy between those two speeds.

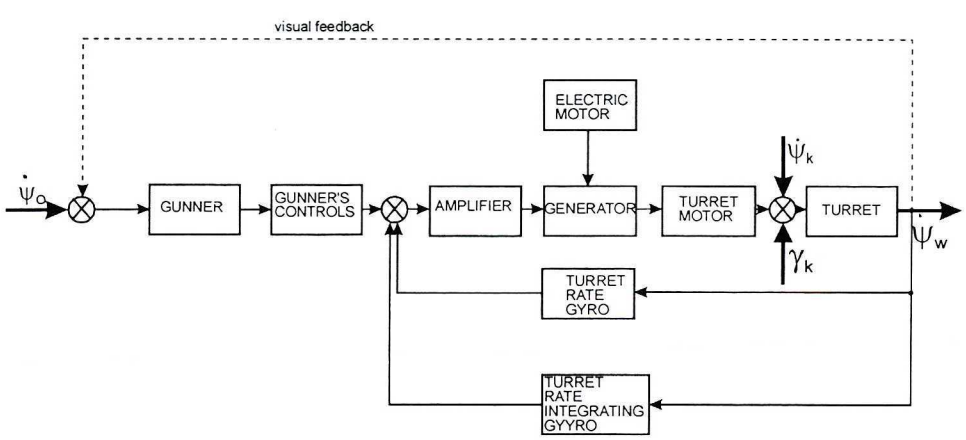

Fig. 2. Block diagram of an azimuth drive with gyro feedbacks

The functional scheme of the tank gun stabiliser is shown in Fig. 3. [7], [8]. The stabiliser is divided into appropriate functional parts:

- **GC**-gunner's controller;
- **FG**- free gyroscope (contains **SCT**- synchro-control-transformer);

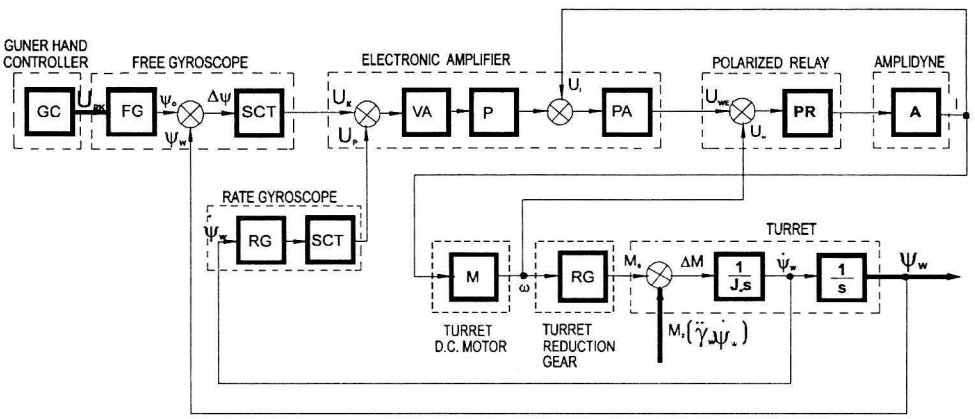

Fig. 3. Functional scheme of investigated azimuth stabiliser

- **RG** – rate gyroscope (contains **SCT**- synchro-control-transformer);
- **EA** – electronic amplifier (contains: **VA**-voltage amplifier, **PA**- power amplifier, **P**-phase sensor);
- **PR** – polarised relay;
- **A** – amplidyne;
- **M** – turret d.c. motor (azimuth drive);
- **RG** – turret reduction gear that drives the turret.

The stabiliser realises the following two basic functions:

- ➢ alteration of the turret angular position with respect to the hull with the aid of gunner hand controler **GC** during aiming at a target and tracking of a target;
- ➢ stabilisation of a given gun turret angular position ψ_W, in the turret thrust bearing plane, in presence of the disturbing torque M_Z caused by the tank movements [9], [10], [11]. The considered movements are: disturbing signal caused by the hall "snake-like" angular vibration ψ_W (motion of the vehicle in yaw) and disturbing signal caused by the hull transversal angular vibration $\gamma_K = \gamma_W$ (motion of the vehicle in roll),

In the operating conditions, tracking and aiming at a target processes occur simultaneously.

3. Experimental investigations

In order to simplify identification, the system was divided into appropriate functional parts. Then, via laboratory tests, dynamic and static characteristics of those parts were obtained and numerical values of coefficients of suitable mathematical model of the system were determined.

3.1. Free gyroscope

The mathematical model of the free gyroscope (FG) assumes that the free gyroscope is a proportional element - due to small viscous friction in bearings and small inertia moments of frames [12], [13], [14], [15], [16].
Block diagram of the measuring system for measurement of the synchro-control-transformer characteristics and the characteristic voltage versus angle of rotation is shown in Fig. 4. [17]. The gyrobox contains the investigated free gyroscope and its synchro-control-transformer (SCT).

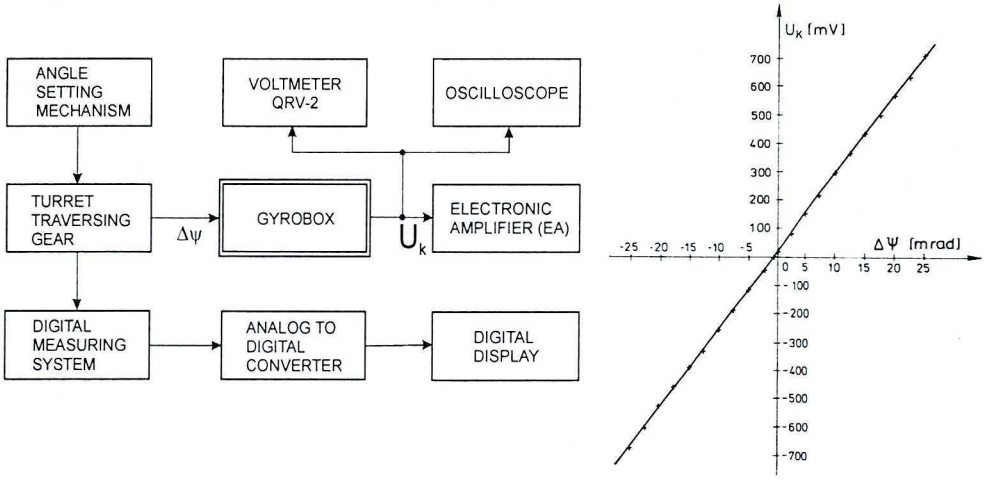

Fig. 4. Block diagram of the measuring system for measurement of the synchro-control-transformer (SCT) characteristics and the characteristic voltage versus angle of rotation

The working range of SCT is ±20 mrad, so we can assume (see Fig. 4) that its characteristic is linear. In further descriptions, the synchro-control-transformer (SCT) will be treated as a proportional element (its gain coefficient has been designated as k_{ST}) due to large difference between frequency of control and frequency of supply voltage (frequency of control is about 1–3 Hz whereas supply voltage frequency is 400 Hz).
During aiming at a target and tracking of a target, the gunner can set, via aiming potentiometer, the aiming torque that influences frames of free gyroscope (FG). Block diagram of the measuring system for measurement of the free gyroscope aiming electromagnet characteristics and the characteristic aiming velocity

versus voltage is shown in Fig. 5. The velocity of precession of the FG frames is proportional to the output voltage from the aiming potentiometer (gunner hand controller in Fig. 3). While aiming, the aiming electromagnet and free gyroscope are treated as an ideal integrator (due to small inertia moment of the frames) [11], [12], [13], [14], [15], [16]. In future descriptions, the gain coefficient of the integrator is designated by k_{EM} .

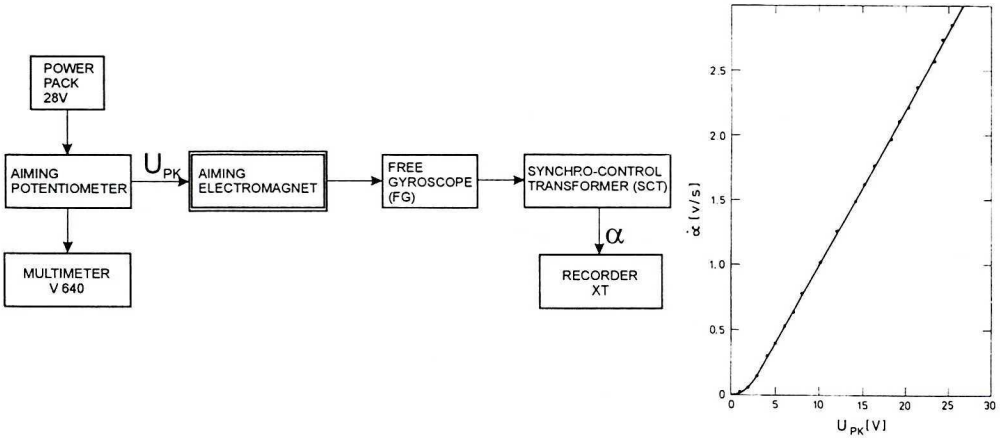

Fig. 5. Block diagram of the measuring system for measurement of the free gyroscope aiming electromagnet characteristics and the characteristic aiming velocity versus voltage

3.2. Rate gyroscope

The rate gyroscope (RG) is treated as an oscillatory element. Numerical values of its time constants T_{01}, T_{02}, T_0 may be found in [11], [12], [13], [14], [15], [16].

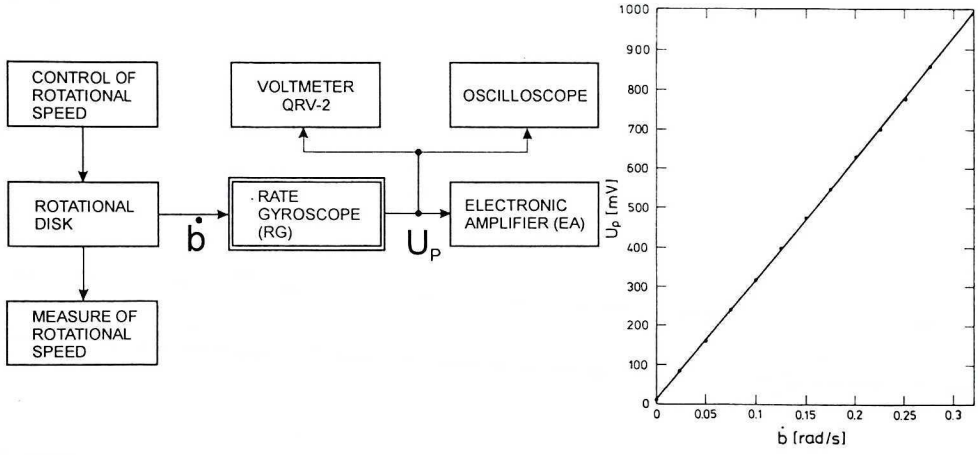

Fig. 6. Block diagram of the measuring system for measurement of the rate gyroscope characteristics and the characteristic voltage versus angular velocity

The block diagram of measuring system for measurement of the rate gyroscope characteristics and characteristic voltage versus angular velocity is shown in Fig. 6. In working range of the rate gyroscope synchro-control-transformer we can assume that the obtained characteristic is linear. In future descriptions, the gain coefficient of rate gyroscope is denoted as k_{SP}.

The differential equation describing the rate gyroscope may be written as

$$T^2{}_{01}\ddot{U}_P + T_{02}\dot{U}_P + U_P - \dot{\psi}_W T_0 k_{SP} = 0. \tag{1}$$

3.3. Electronic amplifier

The electronic amplifier (EA) is treated as a proportional element, due to its small time constants in comparison with time constants of other parts of the considered control system [16]. The block diagram of the measuring system for measurement of the electronic amplifier as well as the polarised relay and the amplidyne characteristics, tested in common, is shown in Fig. 7.

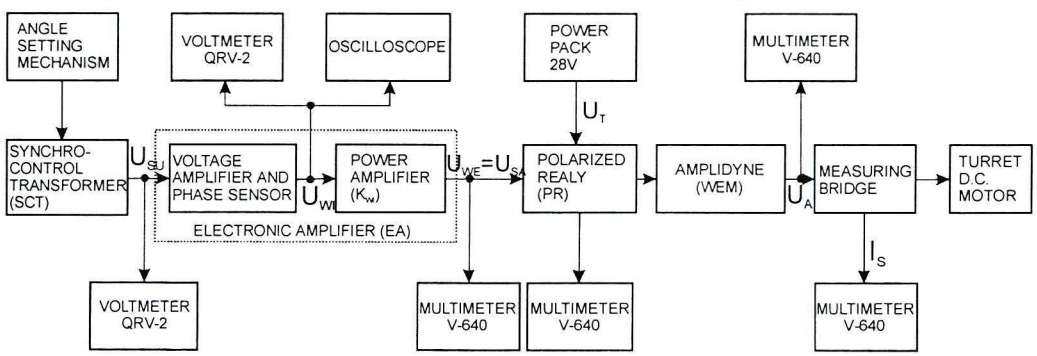

Fig. 7. Block diagram of the measuring system for measurement of the electronic amplifier as well as polarised relay and amplidyne characteristics, tested in common

Taking into account that the current feedback from d.c. motor influences the power amplifier, one determined the characteristic without power amplifier (taken into consideration in the current feedback) and the whole characteristic of the electronic amplifier (Fig.8).

The obtained overal characteristic is non-linear and may be written as [8], [18], [19], [20]

$$U_{SU}K_{W1} - U_{WE} = 0 \quad \text{for} \quad -U_{SU1} \le U_{SU} \le U_{SU1}, \tag{2}$$

where K_{W1} – stands for the gain coefficient of the linear part of characteristic,

$$-1244540U^4{}_{SU} + 444193U_{SU}{}^3 - 60957U_{SU}{}^2 + 4107U_{SU} - 15.7 - U_{WE} = 0 \tag{3}$$

(for) $U_{SU1} \langle U_{SU} \le U_{SU2}$,

$$883004U^4_{SU} + 330272U^3_{SU} + 48863U^2_{SU} + 3635U_{SU} + 10.3 - U_{WE} = 0 \quad (4)$$

$$(for) \quad -U_{SU2} \leq U_{SU} \langle U_{SU1},$$

$$U_{WE} - U_{MWE} = 0 (for) U_{SU} \rangle U_{SU2}, \quad (5)$$

$$U_{WE} + U_{MWE} = 0 \quad (for) \quad U_{SU} \langle -U_{SU2}. \quad (6)$$

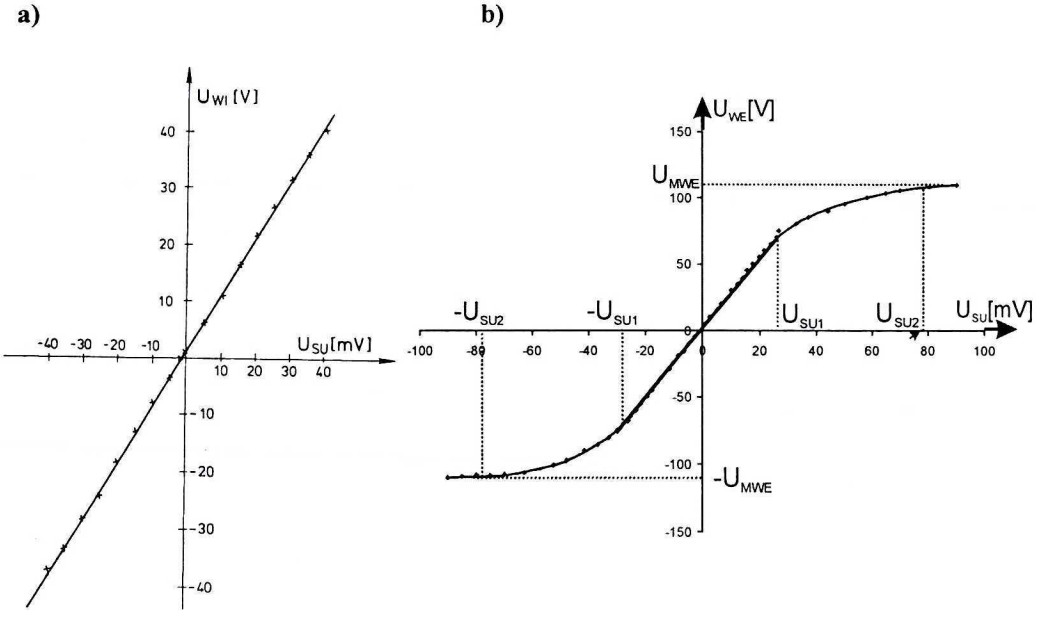

Fig. 8. Characteristics of the electronic amplifier: a) voltage versus voltage (without power amplifier), b) the whole characteristic of the electronic amplifier

3.4. Polarized relay and amplidyne

The polarized relay (PR) and the amplidyne (WEM) were tested in common [20]. For that reason, their mutual internal feedback connections could be omitted. The negative feedback from undercompensation of the amplidyne was introduced at the output of the considered subsystem.

The characteristics of the polarised relay and the amplidyne were determined (Fig. 9) by means of the measuring system shown in Fig. 7.

The obtained voltage versus voltage characteristic is non-linear (Fig. 9a) and may be written as [8], [18], [19], [20]

$$U_{SA} K_{W2} - U_A = 0 (for) - U_{SA1} \leq U_{SA} \leq U_{SA1} \quad (7)$$

where K_{W2} – stands for the gain coefficient of the linear part of the characteristic,

$$0.000311U^6_{SA} - 0.064278U^5_{SA} - 5.50826U^4_{SA} - 250.468U^3_{SA} - 6373.61U^2_{SA} + -86054.3U_{SA} + 481662 - U_A = 0 (for) U_{SA1} \langle U_{SA} \langle U_{SA3} (and) U_A \langle U_{AM}, \quad (8)$$

$$U_A - U_A = 0(for)U_{SA} \geq U_{SA3}(and)U_{SA2}\langle U_{SA}\langle U_{SA3}(and)U_A = U_A \quad , \tag{9}$$

$$-0.000463U^6{}_{SA} - 0.095721U_{SA}{}^5 - 8.21027U_{SA}{}^4 - 373.658U^3{}_{SA} +$$
$$-9516.2U^2{}_{SA} - 128584U_{SA} - 720209 - U_A = 0(for) - U_{SA3}\langle U_{SA}\langle -U_{SA1} \tag{10}$$
$$(\text{and}) \quad U_A\rangle - U_{AM},$$

$$U_A + U_{AM} = 0(for)U_{SA} \leq -U_{SA3}(and) - U_{SA3}\langle U_{SA}\langle -U_{SA2}(and)U_A = U_{AM} . \tag{11}$$

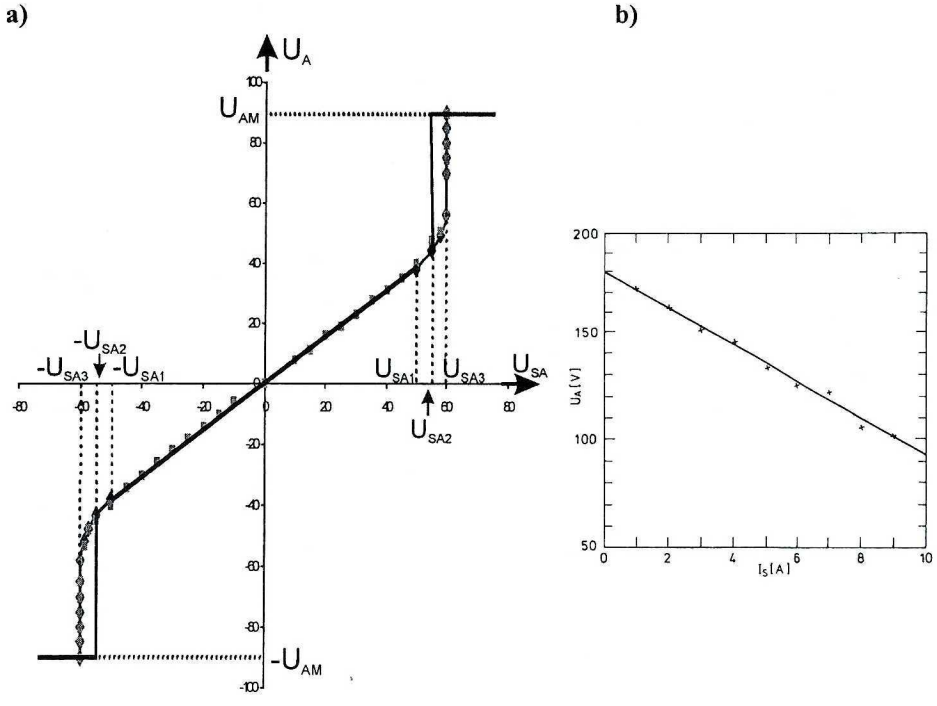

Fig. 9. Characteristics of the polarised relay and amplidyne, tested in common: a) voltage versus voltage, b) voltage versus current

The voltage versus current characteristic was used to obtain the coefficient of undercompensation of the investigated polarised relay and amplidyne, tested in common. The coefficient is denoted as R_β.

The step response of the polarised relay and the amplidyne has been measured using an oscilloscope with memory (Fig. 10). In result, it has been found that the investigated object may be treated as an oscillatory element and its differential equation may be written as [13], [21], [22]

$$T_1\ddot{E}_A + T_2\dot{E}_A + E_A - U_A = 0 . \tag{12}$$

The numerical values of the time constants T_1, T_2 have been found using appropriate methods [23], [24].

3.5. Turret d.c. motor

The experimental investigations of the turret d.c. motor were carried out by means of a special measuring system (Fig. 10).

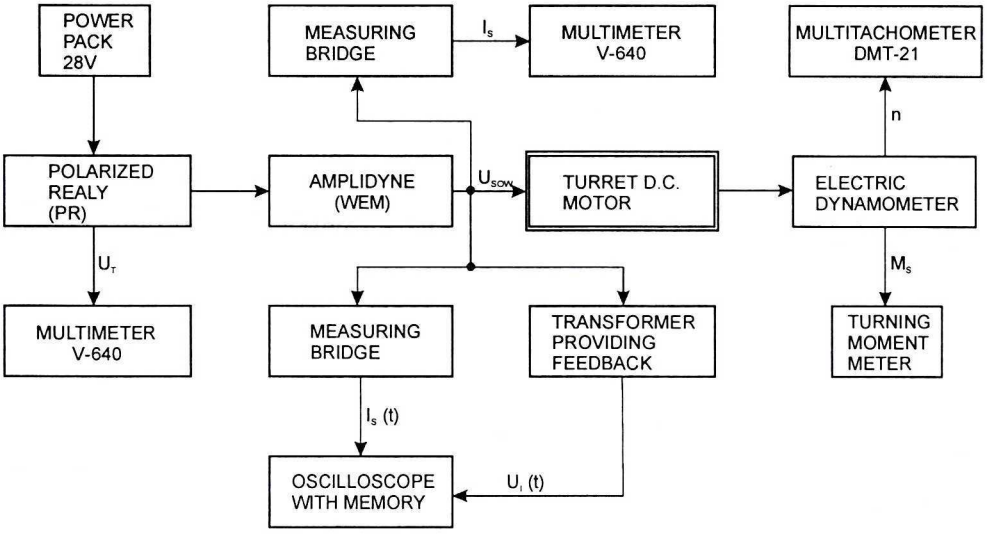

Fig. 10. Block diagram of the measuring system for measurement of the turret d.c. motor and the tachometer feedback characteristics

The obtained characteristics of the turret d c motor and of the tachometer feedback voltage versus rotational speed, and so are the characteristic of the turret d c motor torque versus current are linear (Fig. 11). In future descriptions, the gain coefficients of the turret d c motor are denoted as k_E, k_T, k_m respectively.

The resistance of the rotor was measured and its coefficient K_S was also found.

The step response of the turret d.c. motor was measured using an oscilloscope with memory (Fig. 10). It was found that the investigated object could be treated as an inertial element, and its differential equation could be written as [13], [21], [22].

$$T_S \dot{I}_S - U_{SOW} K_S + I_S = 0 \tag{13}$$

The numerical value of the time constant T_S was found using appropriate methods [23], [24].

Applying an oscilloscope with memory, one registered the output functions of d.c. motor current and voltage of current feedback. In result, the coefficient R_I was found (see Fig. 12).

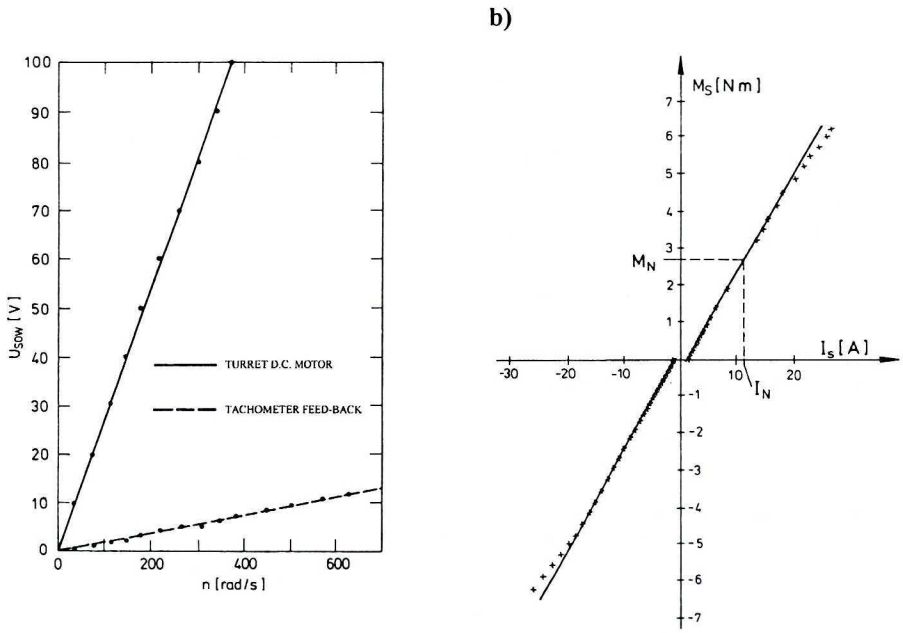

Fig. 11. The characteristics of the turret d c motor and of the tachometer feedback voltage versus rotational speed (a) and the characteristic of the turret d c motor torque versus current (b)

3.6. Turret reduction gear and turret with gun

The turret reduction gear (RG) was treated as rigid and its backlashes are neglected. The inertia moment of the turret reduction gear was reduced to the shaft of the turret d.c. motor (the transmission ratio of azimuth drive). Numerical values of coefficients are denoted as J_{SR}, i_r [20] (see Fig. 12).

The tank's turret and gun are treated as a rigid body with total mass m_W. The turret moment of inertia with respect to the vertical axis of rotation is denoted as J_W. Angular displacements of turret and gun (while stabilising the position of the gun) in fact are very small (about 3 mrad), so the Cartesian coordinates are used to describe the bending of the main armament [3], [10], [25].

The torque acting on the turret in dependence upon the moment of inertia may be written as follows:

$$M_W = J_W \ddot{\psi}_W , \tag{14}$$

where:

J_W – the turret moment of inertia with respect to the vertical axis of rotation;

$\ddot{\psi}_W$ – the turret angular acceleration in yaw.

Total damping torque between the hull and the turret consists of the following torques:

M_T – the torque acting on the turret due to the coulomb friction between the

turret and the hull (mainly in the turret ball bearing);

M_{JR} – the torque acting on the turret due to the moment of inertia of the azimuth drive system (motor's rotor and gear box's inter-mating gears);

The components of the total friction torque between the hull and the turret can be defined as follows:

$$M_T = M_{ST} sign(\dot{\psi}_K - \dot{\psi}_W) = M_{ST} sign\dot{\psi}_{KW} \tag{15}$$

$$M_{JR} = J_{SR} i_r^2 \ddot{\psi}_{KW} \tag{16}$$

where:

M_{ST} – static torque of friction;

$\dot{\psi}_K, \dot{\psi}_W$ – the hull and the turret angular velocity in yaw;

$\dot{\psi}_{KW}, \ddot{\psi}_{KW}$ – relative velocity and acceleration of the turret (relative to the hull);

J_{SR} – the moment of inertia of azimuth drive motor's rotor and gear box with respect to the axis of rotation;

i_r – the azimuth drive transmission ratio.

The turret centre of gravity (TCG) is moved to fore-part of the turret due to thick front armour and heavy main gun.

In many cases, accelerations of the TCG in roll (as less important) can be omitted [3], [10], [25]. Then, the total moment due to non-balance of the turret M_γ (angular displacements of turret γ_W while stabilising the position of the gun are very small) can be defined as follows:

$$M_\gamma = m_W y_{TCG} z_{TCG} \ddot{\gamma}_W + m_W g y_{TCG} \gamma_W \tag{17}$$

where:

m – the total mass of the turret;

g – accelerations of gravity;

y_{TCG} – the distance of the TCG from the turret axle of rotation;

z_{TCG} – the distance of the TCG from the hull axle of rotation;

$\gamma_W = \gamma_K$ – angular displacement of the turret and the hull in roll.

To simplify the structural scheme of the stabilised main armament, we apply the following relations:

$$K_{NW} = m_W g y \quad , \tag{18}$$

$$T_{NW} = \frac{z_{TCG}}{g} . \tag{19}$$

The parameters J_W, J ,i, M_T, m_W, y_{TCG}, z_{TCG} were found in [13], [14], [16], [20]. The results of the investigations lead to the conclusion that most of the static characteristics are linear or almost linear. Strong nonlinearities that are included in the mathematical model of the system resulted from:

- coulomb friction forces between the gun turret and the hull,
- electronic amplifier saturation,

– saturation and hysteresis loop of the polarised relay and amplidyne (treated in common).

4. Mathematical model

The structural scheme of the overall system (with three inputs and one output) [7], [8], [26], [27], [28], [29] – see Fig. 12, was derived on the basis of the obtained static characteristics and transfer functions of individual parts of the system, and based on the knowledge about the system feedbacks.

The input signals are:

U_{PK} – the reference signal given by the operator,

ψ_K – the disturbing signal caused by the hull "snake-like" movements,

γ_K – the disturbing signal caused by the transversal angular displacements of the hull around the longitudinal axis.

The gun turret angular displacement ψ_w represents the output signal.

The mathematical model was formulated on the following assumptions:

– the free gyroscope (FG) was treated as a proportional element (due to small viscous friction in bearings and small inertia moments of frames);

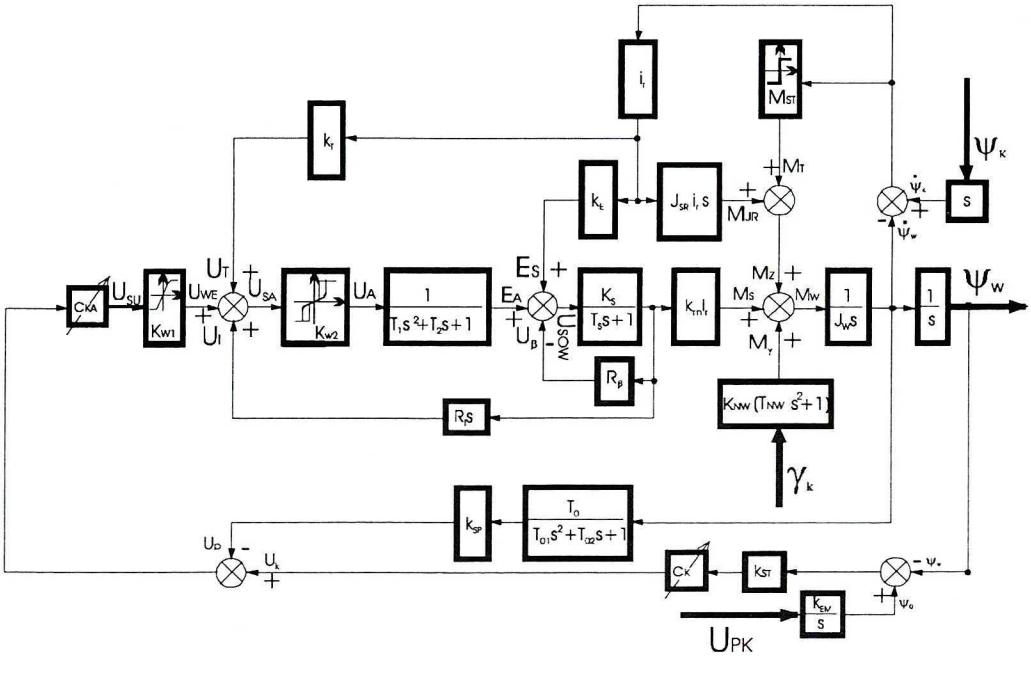

Fig. 12. Non-linear model of the investigated stabiliser

– the aiming electromagnet of the free gyroscope was assumed to be an ideal integrator (due to small inertia moments of frames);

– the synchro-control-transformer (SCT) was treated as a proportional element (due to large difference between the frequency of control and the supply voltage);
– the electronic amplifier (EA) was treated as a proportional element (due to small time constants);
– the polarised relay (PR) and amplidyne (A) were tested in common. For that reason, their mutual internal feedback connections could be omitted. The negative feedback from undercompensation of the amplidyne was introduced at the output of the considered subsystem;
– the turret reduction gear was treated as a rigid one and its backlashes was omitted;
– the inertia moment of the turret reduction gear was reduced to the shaft of the d.c. motor.

A computer simulation method was applied for the investigation of the considered control system. On the basis of the mathematical model, an algorithm and computer program was worked – out. Making use of the Matlab–Simulink program, one worked-up a scheme for numerical computations. The computer program facilitates:
– the choice of the stabiliser operating range (stabilisation or aiming at a target);
– the choice and generation of input signals (U_{PK}, γ_K, ψ_K) including disturbances, in the form of harmonic functions or their parts and rectangular pulses;
– generation of non-linear characteristics;
– solving the system equations via the Runge-Kutta method (at given initial conditions for angular position and velocity of the gun-turret);
– graphical illustration of input and output time signals.

5. Verification of mathematical model

The mathematical model and its numerical implementation were experimentally verified. To this aim:
– the results of model testing (for open-loop system) were compared with the existing results of experimental tests carried-out on a real plant [30];
– tests of the complete closed-loop system were carried out and their results were compared with the results of numerical computations [20].

The results of experimental and model testing carried out on the open – loop system (without feedbacks realised by rate gyroscope and free gyroscope) are shown in Fig. 13 and Fig. 14. The step and frequency responses were obtained for voltages (amplitude of step and harmonic functions) 10V, 15V, 20V supplying the aiming electromagnet.
The differences between step responses for different polarisation of voltage are greater than those between step responses obtained from the model and experimental testing. The same holds for frequency responses.

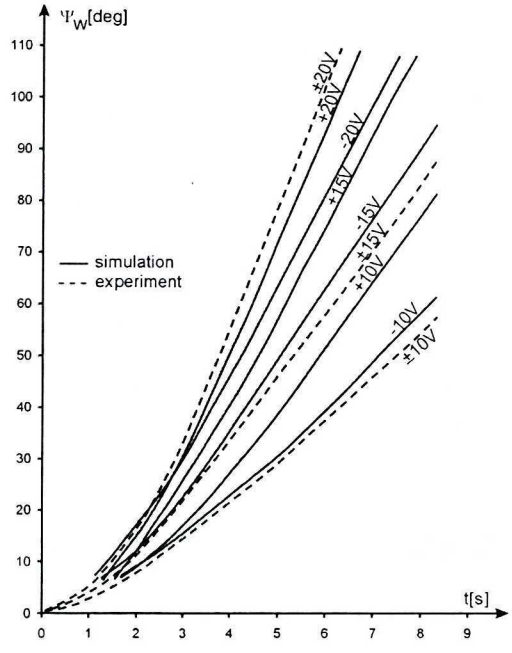

Fig. 13. Step responses for open – loop system

The tests of the complete closed – loop system were the next stage of mathematical model verification. Experimental testing was carried – out on the stand representing the investigated tank gun stabiliser (Fig. 15). All functional parts of the stand were original, like in a real tank.

The inertia moment of the turret and gun was imitated by special flywheel and reduction gear. The torque of friction between turret and hull was controlled to obtain similar values as in a real tank. The effects of vehicle motion on the turret, under typical conditions of tank operating over rough ground (motion in yaw), were imitated by input function mechanism. Generation of input signals applied to aiming electromagnet was possible, as well.

The investigations were carried out for two types of signals. The first of them was the reference signal given by the operator (U_K) as an rectangular impulse of voltage U_i=10V, 20V, 27.5V. The impulse responses are shown in Fig. 16.

The second type of signal was the disturbing signal caused by the hull "snake-like" movements (ψ_K) for various amplitudes and frequencies of the input functions.

Figur 17 shows attenuation diagrams for various regulation potentiometers settings c_K and c_{KA}.

The results of experimental and model simulation investigations show that the mathematical model and its numerical implementation were worked-out correctly.

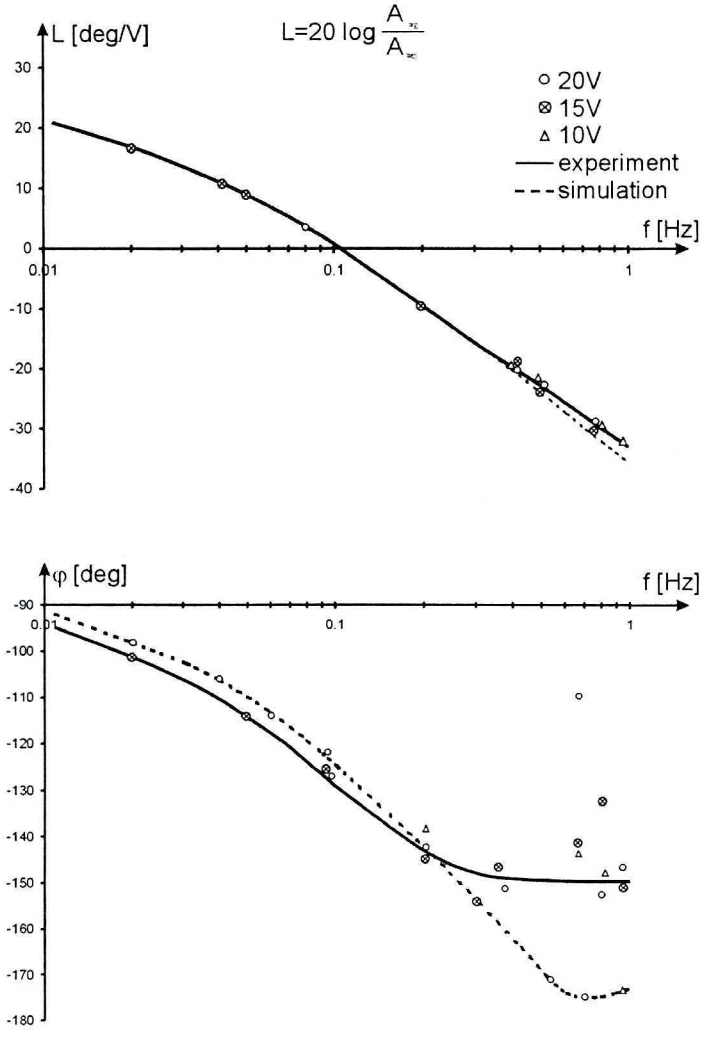

Fig. 14. Frequency responses for open – loop system

6. Concluding remarks

The author is of the opinion that the proposed methodology of simulation investigations represents a sufficient level of generality. It comprises a complex analysis of the gun-turret stabilisation system, beginning from identification of individual functional parts of the system, through the algorithm for the mathematical model up to detailed investigation of system properties.

The mathematical model and its numerical implementation have been experimentally verified. To this aim, the results of model testing (for open-loop system) were compared with the existing results of experimental tests carried-out on a real plant [30], and tests of the complete closed-loop

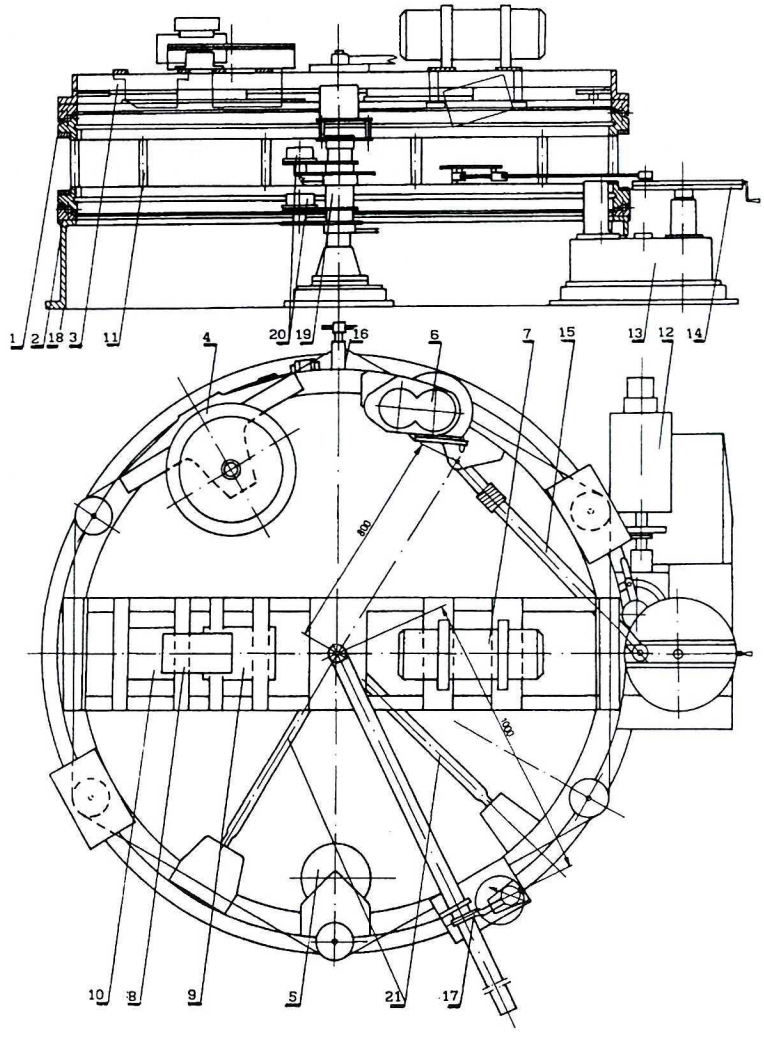

Fig.15. The stand of the investigated tank gun stabiliser
1 – turret axial bearing (between turret and hull), 2 – hull axial bearing (between hull and base), 3 – frame (imitating the turret of tank) for parts of stabiliser fitting up, 4 – flywheel and reduction gear (imitated the inertia moment of turret), 5 – balance weight of flywheel, 6 – turret reduction gear and dc motor, 7 – amplidyne, 8 – motor-generator set, 9 – electronic amplifier, 10 – gyro box, 11 – frame imitating the hull of tank, 12 – three phase motor for generation of input function caused on the hull, 13 – reduction gear of input function mechanism, 14 – mechanism for amplitude of input function setting, 15 – connecting-rod between input function mechanism and frame imitating the hull of tank, 16 – moment of friction, between turret and hull, controller, 17 – lever for moment of friction measurement, 18 – base of stand, 19 – base of electro-optical converter tubes for angle of rotation measurement, 20 – electro-optical converter tubes (CPPC50), 21 – levar between CPPC50 and hull as well as between CPPC50 and turret

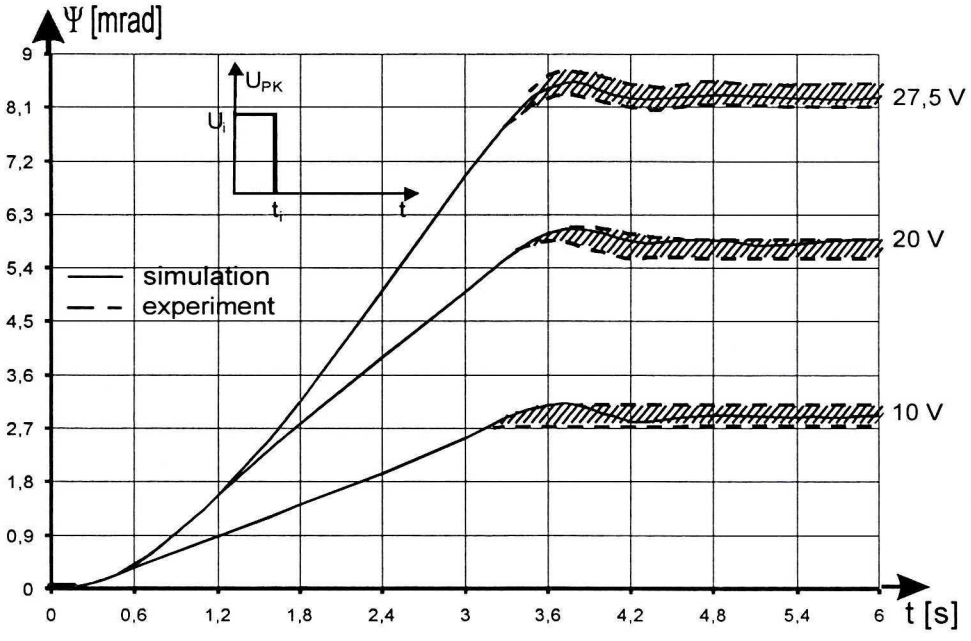

Fig. 16. Impulse responses of tank gun stabiliser

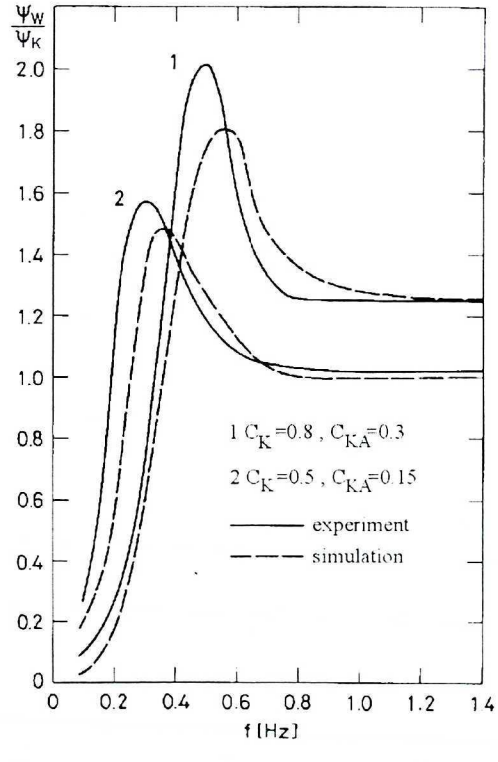

Fig. 17. Attenuation diagrams of tank gun stabiliser

system [20] were carried-out, and their results were compared with the results of numerical computations. The results of experimental and model simulation investigations showed that the mathematical model and its numerical implementation were correctly developed.

The considered mathematical model may be generalised in a simple way for the case of random signals representing disturbances.

In the next stage of the work, the following tests should be carried-out:

- using the described above mathematical model of the system to perform simulation investigations of the influence of regulation potentiometers settings c_K and c_{KA} on the exactness of stabilisation and transient processes quality (i.e., setting time and magnitude of the first over-regulation);
- analysis of possibilities of improving performance characteristics of the stabiliser via changing internal feedbacks' gain coefficients;
- analysis of influence of amplitude and frequency of disturbing inputs (propagated from the hull on the gun-turret) on the exactness of stabilisation at a given position;
- analysis of possibilities of introducing additional feedbacks' in the investigated system.

Manuscript received by Editorial Board, February 15, 2002;
final version, June 15, 2002.

REFERENCES

[1] Czołg śretni T-55A i czołg dowódczy T-55AD. Opis i użytkowanie. MON, Panc.Sam. 46/68.

[2] Krupka R.M., Mathematical simulation of the dynamics of military tank. SAE, Technical paper series, International congress & exposition, Detroit, Michigan 1985.

[3] Tokarzewski J., Papliński K., Juszczyk A., Sobczyk Z.: Urządzenia elektryczne i osprzęt pojazdów mechanicznych. Część II: Układy stabilizacji uzbrojenia wozów bojowych. Skrypt WAT, Warszawa 1999.

[4] Papliński K., Rybak P.: Rozwój systemów zwiększających siłę ognia prowadzonego z armaty czołgowej, Zeszyty Naukowe WSO WP nr 1 (09), Poznań 2001, pp. 75÷93.

[5] Juszczyk A., Papliński K., Sobczyk Z.: Układy stabilizacji uzbrojenia wozów bojowych. Zeszyty Naukowe AON, Nr 4/96, Rembertów 1996, pp. 260÷275.

[6] Papliński K., Sobczyk Z.: The tank gun elevation stabiliser as a second - order multi-loop servomechanism, UEES'99, St. Petersburg (Russia) 1999, Vol. 3, pp. 1377÷1382.

[7] Papliński K.: Modelling and simulation of a multi-loop servomechanism. AVCS'98, Amiens (France) 1998, pp.57÷62.

[8] Borkowski W., Papliński K.: Simulation of a second-order multi-loop servomechanism. International Conference MMAR'94 , Międzyzdroje 1994, pp.221÷226.

[9] Papliński K., Sobczyk Z., Tokarzewski J.: Badanie obciążeń dynamicznych działających na uzbrojenie czołgu, II Konferencja Odporność Udarowa Konstrukcji, Rynia 1998, pp. 267÷276.

[10] Papliński K.: Uzbrojenie czołgu jako obiekt regulacji dla układu stabilizacji położenia kątowego, Archiwum Motoryzacji Nr1-2, PWN Warszaw 2001, str. 19÷30.
[11] Никитин А.О., Сергеев Л.В., Тарасов В.В.: Теоря танка, Москва 1956.
[12] Корнэзв В.В.: Электроавтоматика и электрооборудование танков. Москва 1964.
[13] Корнэзв В.В.: Основы автоматики и танковые автоматичэскиэ систэмы. Москва 1976.
[14] Белановски А.: Электроавтоматика и электрооборудование танков. Москва 1963.
[15] Бесекерски В.А., Попов Э.П.: Теоря системов автоматического регулирования. Москва 1975.
[16] Бесекерски В.А.: Динамический анализ системов автоматического регулирования. Москва 1970.
[17] Missala J., Missala T.: Elektryczne pomiary wielkości mechanicznych. PWN, Warszawa 1971.
[18] Papliński K., Sobczyk Z.: Modelling of a tank gun stabiliser. IASTED International Conference, Innsbruck, Austria 1997 pp.186÷189.
[19] Papliński K.: Modelling of a Nonlinear Second-Order Multi-Loop Servomechanism, IASTED International Conference, Grindewald, Switzerland 1998 pp.18÷21.
[20] Papliński K.: Badania możliwości polepszenia układu stabilizacji wieży czołgowej. Rozprawa doktorska, Warszawa 1994.
[21] Gibson J. E., Tuteur F. B.: Człony układów regulacji, WNT, Warszawa 1961.
[22] Kaczorek T.: Teoria sterowania. PWN, Warszawa, T.1 1977, T.2 1981.
[23] Pląskowski A.: Eksperymentalne wyznaczanie własności dynamicznych obiektów regulacji. WNT, Warszawa 1965.
[24] Bubnicki Z.: Identyfikacja obiektów sterowania. PWN, Warszawa 1974.
[25] Burdziński Z.: Teoria ruchu pojazdu gąsienicowego. WKŁ, Warszawa 1972.
[26] Borkowski W., Papliński K.: Simulation of a second-order multi-loop servomechanism, sympozium MMAR'95, Międzyzdroje 1995 pp. 389÷394.
[27] Papliński K., Tokarzewski J.: Badania symulacyjne układu stabilizacji położenia kątowego wieży wozu bojowego. Konferencja Kazimierz Dolny'97, Kazimierz Dolny 1997 pp. 141÷146.
[28] Borkowski W.: Dynamiczna analiza konstrukcji metodą elementów skończonych. Dodatek do Biuletynu Nr.5 (381) WAT, Warszawa 1984.
[29] Borkowski W., Konopka S., Prochowski L.: Dynamika maszyn roboczych. WAT, Warszawa 1992.
[30] Paszkowski S.: Analiza przyczyn niedokładnej pracy automatyki czołgu oraz ustalenie wniosków i zaleceń. Sprawozdanie z pracy naukowo-badawczej, Warszawa 1967.

Badania eksperymentalne i identyfikacyjne stabilizującego i śledzącego układu sterowania

Streszczenie

Przedmiotem rozważań jest czołgowy stabilizator położenia kątowego armaty w płaszczyźnie poziomej (w azymucie). W wyniku upraszczającej identyfikacji układ został podzielony na odpowiednie człony funkcjonalne. Następnie w wyniku badań laboratoryjnych wyznaczone zostały charakterystyki dynamiczne i statyczne jak również wartości liczbowe odpowiednich

współczynników modelu matematycznego. Na bazie wyznaczonych charakterystyk statycznych i transmitancji operatorowych poszczególnych modułów układu oraz na podstawie znajomości związków funkcjonalnych pomiędzy nimi, zbudowano schemat funkcjonalny powyższego układu. Do badań rozważanego układu sterowania została zastosowana komputerowa metoda badań symulacyjnych. Model matematyczny i program badań symulacyjnych zostały zweryfikowane eksperymentalnie.

W tym celu:

- wyniki badań modelowych (dla układu bez sprzężeń zwrotnych) zostały porównane z wynikami badań eksperymentalnych przeprowadzonymi na obiekcie rzeczywistym;
- zostały przeprowadzone badania pełnego układu ze sprzężeniami zwrotnymi i ich wyniki zostały porównane z wynikami badań symulacyjnych.

Wyniki badań eksperymentalnych i modelowych badań symulacyjnych wykazały że, model matematyczny i program badań symulacyjnych zostały zbudowane poprawnie a uzyskane wyniki są porównywalne.